Roth, R. A., & Cassell, M. P. (1983) *Science (Washington, D.C.) 219*, 299–301.
Roth, R. A., Mesirow, M. L., & Cassel, D. J. (1983) *J. Biol. Chem. 258*, 14456–14460.
Russo, M. W., Lukas, T. J., Cohen, S., & Staros, J. V. (1985) *J. Biol. Chem. 260*, 5205–5208.
Shia, M. A., & Pilch, P. F. (1983) *Biochemistry 22*, 717–721.
Shia, M. A., Rubin, J. B., & Pilch, P. F. (1983) *J. Biol. Chem. 258*, 14450–14455.
Stadtmauer, L., & Rosen, O. M. (1986) *J. Biol. Chem. 261*, 10000–10005.
Tamura, S., Fujita-Yamaguchi, Y., & Larner, J. (1983) *J. Biol. Chem. 258*, 14749–14752.
Ullrich, A., Coussens, L., Hayflick, J. S., Dull, T. J., Gray, A., Tam, A. W., Lee, J., Yarden, Y., Libermann, T. A., Schlessinger, J., Downward, J., Mayes, E. L. V., Whittle, N., Waterfield, M. D., & Seeburg, P. H. (1984) *Nature (London) 309*, 418–425.
Ullrich, A., Bell, J. R., Chen, E. Y., Herrera, R., Petruzzelli, L. M., Dull, T. J., Gray, A., Coussens, L., Liao, Y.-C., Tsubokawa, M., Mason, A., Seeburg, P. H., Grunfeld, C., Rosen, O. M., & Ramachandran, J. (1985) *Nature (London) 313*, 756–761.
Van Obberghen, E., Rossi, B., Kowalski, A., Gazzano, H., & Ponzio, G. (1983) *Proc. Natl. Acad. Sci. U.S.A. 80*, 945–949.
White, M. F. & Kahn, C. R. (1986) *Enzymes (3rd Ed.) 17*, 247–310.
White, M. F., Haring, H. U., Kasuga, M., & Kahn, C. R. (1984) *J. Biol. Chem. 259*, 255–264.
White, M. F., Takayama, S., & Kahn, C. R. (1985) *J. Biol. Chem. 260*, 9470–9478.
Yip, C. C., Yeung, C. W. T., & Moule, M. L. (1978) *J. Biol. Chem. 253*, 1743–1745.
Yu, K.-T., & Czech, M. (1984) *J. Biol. Chem. 259*, 5277–5286.
Zoller, M. J., Nelson, N. C., & Taylor, S. S. (1981) *J. Biol. Chem. 256*, 10837–10842.

Stratum Corneum Lipid Phase Transitions and Water Barrier Properties

Guia M. Golden, Donald B. Guzek, Alane H. Kennedy, James E. McKie, and Russell O. Potts*
Pfizer Central Research, Groton, Connecticut 06340
Received September 19, 1986; Revised Manuscript Received December 17, 1986

ABSTRACT: In mammals, the outer skin layer, the stratum corneum, is the ultimate barrier to water loss. In order to relate barrier function to stratum corneum structure, samples from porcine skin were investigated by using differential scanning calorimetry (DSC), infrared (IR) spectroscopy, and water permeability techniques. Results of DSC and IR studies show that stratum corneum lipids undergo thermal transitions between 60 and 80 °C similar to lipid thermotropic transitions seen in a variety of synthetic and biological membranes. Results of water flux experiments performed under conditions similar to those of the DSC and IR studies show an abrupt change in permeability at about 70 °C. At low temperatures, water flux values are similar to those obtained for human skin in vivo, yielding an activation energy of 17 kcal/mol, in excellent agreement with values obtained for water flux through a variety of lipid biomembranes. In contrast, at temperatures above about 70 °C, water flux is characterized by an activation energy only slightly higher than that of free diffusion, suggesting that the stratum corneum offers little diffusional resistance under these conditions. These combined results suggest that increased disorder in stratum corneum lipid structure, brought about by thermotropic transitions, results in dramatically altered diffusional resistance of this tissue to water flux. Thus, as found for numerous biological membranes, water flux and lipid order in porcine stratum corneum are inversely related.

The mammalian stratum corneum, the outermost layer of the skin, is a unique structural composite which forms the ultimate barrier between life and the surrounding environment. This layer is comprised of protein-rich cells embedded in a lipid matrix in a manner reminiscent of "bricks in mortar" (Michaels et al., 1975). Recently, a more sophisticated view of the stratum corneum has emerged showing corneocyte cells, composed primarily of the protein keratin, surrounded by a three-dimensional, multilamellar lipid domain (Elias, 1982: Wertz & Downing, 1982). Furthermore, evidence suggests that cholesterol and lipids with long saturated acyl chains (e.g., free fatty acids and ceramides) predominate in the barrier layer (Bowser & White, 1985; Elias et al., 1977), precisely those lipid classes which have been shown to be most effective in forming synthetic and biological membranes of low water permeability (Chapman, 1975; Stubbs, 1983).

One of the most vital functions of the stratum corneum is the regulation of water flux through the skin. For example, removal of the stratum corneum results in an approximate hundredfold increase in water flux (Onken & Moyer, 1963; Scheuplein & Blank, 1971). Lipids play an important role in stratum corneum water barrier function as demonstrated by in vivo and in vitro results showing that treatment of the skin with lipid extractants resulted in dramatically increased water flux (Blank, 1952; Onken & Moyer, 1963; Smith et al., 1982), approaching values obtained after removal of this barrier layer. More recently, Elias and co-workers (Elias et al., 1981) have shown that regional variation of stratum corneum water flux in humans appears to be related to the amount of lipid at each test site, with flux and lipid content varying inversely. While these results suggest the importance of lipids in barrier function, they provide little information about stratum corneum lipid structure. Recently, the stratum corneum has been studied by using differential scanning calorimetry (DSC) and infrared (IR) spectroscopy, techniques which have been used previously to study lipid and protein transitions in a variety of biological and synthetic systems [see Golden et al. (1986) and the references cited therein]. Results

0006-2960/87/0426-2382$01.50/0

obtained with human (Golden et al., 1986), porcine (Golden et al., 1987), and murine (Knutson et al., 1985) stratum corneum samples show that DSC and IR techniques provide independent yet complementary information on the structure of lipid hydrocarbon chains.

In this report, we have combined DSC and IR techniques with in vitro water flux measurements, all performed under similar conditions, to relate changes in stratum corneum lipid structure to water flux through this barrier.

Materials and Methods

Stratum Corneum Preparation. Porcine skin was obtained from a local abattoir. Thoracic skin was removed with a dermatome to a depth of 350 μm within a few minutes of sacrifice of the animal. This tissue was kept on ice for several hours prior to enzymatic treatment to remove the stratum corneum from the underlying tissue. Pieces of skin, cut to about 2 × 2 cm squares, were incubated, stratum corneum side up, on filter paper saturated with 0.5% trypsin (type II, Sigma Chemical Co.) in phosphate-buffered saline at pH 7.4. Following overnight incubation at 22 °C, the stratum corneum and a few adherent epidermal cells were peeled away from the underlying tissue with forceps. The sample was then soaked in 0.01% soybean trypsin inhibitor (Sigma Chemical Co.) for 10 min and gently agitated in distilled water to remove any remaining epidermal cells. Finally, the sample was spread on a wire mesh to dry and stored in a dry atmosphere until used.

Corneocyte Membrane Preparation. The method of Matoltsy and Matoltsy (1966) was used to prepare corneocyte membranes via keratin extraction with alkali. Samples of porcine stratum corneum sheets were cut into small pieces, suspended in 0.1 M sodium hydroxide, shaken with glass beads for 48 h at 5 °C, and centrifuged at 3500 rpm for 10 min. The pellet was resuspended in NaOH for 48 h, with four changes of alkali. The membranes were collected by centrifugation at 3500 rpm at 5 °C, washed 3 times with distilled water, and dialyzed for 48 h against four changes of distilled water. Unlike the Matoltsy and Matoltsy method, however, the sample was not subjected to lipid extraction prior to investigation.

Differential Scanning Calorimetry (DSC). DSC data were obtained as described previously (Golden et al., (1986). In brief, a stratum corneum sample of approximately 10 mg dry mass was hydrated at 22 °C and 75% relative humidity (rh) in a closed chamber containing a saturated solution of NaCl. After several days in this atmosphere, the sample was sealed in a sample cell and heated at 0.75 °C/min from ambient temperature to about 120 °C in a differential scanning calorimeter (Model MC-1, Microcal, Inc., Amherst, MA). Gravimetric analysis of the samples immediately prior to DSC experiments showed an average water uptake of 0.15 g/g of dry stratum corneum. Alternatively, samples were placed in an atmosphere of greater than 95% relative humidity and allowed to absorb a desired mass of water.

Infrared Spectrometry (IR). Infrared spectra were obtained as described previously (Golden et al., 1986). In brief, a sample of stratum corneum approximately 5 cm in diameter was allowed to equilibrate for several days in an environmental chamber maintained at 22 °C and 75% rh. While still in the chamber, the sample was sealed between IR-transparent windows using water-tight and heat-insensitive tape. Once removed from the chamber, the sealed sample was placed in a heating mantle (Barnes Analytical, Stamford, CT) in a Fourier transform infrared (FTIR) spectrometer (Analect Model FX-6200, Laser Precision Corp., Irvine, CA). The temperature of the heating mantle was controlled by using a programmable controller (Omega Instruments, Stamford, CT) and measured by using a thermocouple in contact with the sample holder.

During each experiment, the sample was heated from about 20 to 120 °C in 6–8 h time. During data collection periods, 64 spectral scans were averaged in about 3 min while the temperature remained constant to within ±1 °C. The FTIR instrument was interfaced with a personal computer where the temperature dependence of the peak frequency and half-bandwidth were calculated from digitized data using a center of gravity algorithm (Cameron et al., 1982).

Flux of Tritiated Water (HTO) Vapor. Flux of water vapor through stratum corneum was measured by the method of Blank and co-workers (Blank et al., 1984). A sheet of stratum corneum about 2 × 2 cm was mounted between two diffusion half-cells with the outer surface of the sample mounted toward the donor chamber of the assembled apparatus. Each side of the assembled apparatus had a reservoir sealed with a vapor-tight, septum top and contained 2 mL of a saturated aqueous solution of NaCl and a few hundred milligrams of excess solid. The design of the apparatus was such that the stratum corneum sample only came in contact with the vapor above the liquid. Sodium chloride was chosen since saturated solutions of this salt produce an ambient relative humidity near 75% over the temperature range of 10–90 °C. Thus, stratum corneum samples were maintained at constant relative humidity during all experiments.

The assembled diffusion cells with stratum corneum samples were placed in constant-temperature bath at the desired temperature and allowed to equilibrate for a least 48 h. At the end of this period, the flux experiment was initiated by the introduction, through the septum top, of approximately 1.5 × 10^6 dpm of tritiated water (HTO) into the saturated salt solution on the donor side. Samples (10 μL) were periodically withdrawn from the solutions on both the donor and receiver side and counted in a liquid scintillation counter.

Following an initial lag time, the amount of HTO appearing on the receiver side was linear with time for the duration of the experiment. The experiment was terminated when greater than 5% of the initial HTO was detected in the receiver solution. From a least-squares analysis of the linear portion of the HTO vs. time graph, the rate of appearance of HTO on the receiver side was determined (dpm per hour). This value, when divided by the initial concentration of HTO on the donor side (dpm per cubic centimeter) and the area of the stratum corneum available for diffusion (1.27 cm^2 in these experiments), yields the permeability constant (centimeters per hour) for the diffusion of HTO through the sample. All flux experiments were performed in triplicate for each sample at each temperature.

Results

Figure 1 shows the infrared spectra of porcine stratum corneum in the carbon–hydrogen bond (C–H) stretching region between 2800 and 3000 cm^{-1} for a sample equilibrated at 75% relative humidity and 22 °C. The two traces show spectra obtained when the sample was heated to 30 and 115 °C. These results show that upon heating, the C–H symmetric (near 2850 cm^{-1}) and antisymmetric (near 2920 cm^{-1}) stretching vibrations broaden and shift to higher wavenumber. Figure 2 shows the change in wavenumber of the C–H antisymmetric peak as a continuous function of temperature. These data show that while there is a general increase in wavenumber over the entire temperature range, the increase is particularly dramatic between 60 and 80 °C. Similar results were obtained for the thermal dependence of the peak width,

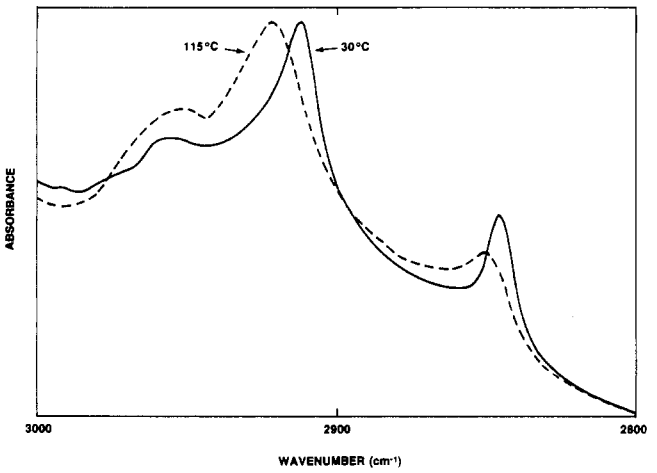

FIGURE 1: Infrared spectra of porcine stratum corneum in the C–H stretching region between 2800 and 3000 cm^{-1}. The spectra were obtained with a sample hydrated at 22 °C and 75% rh and then heated to 30 and 115 °C.

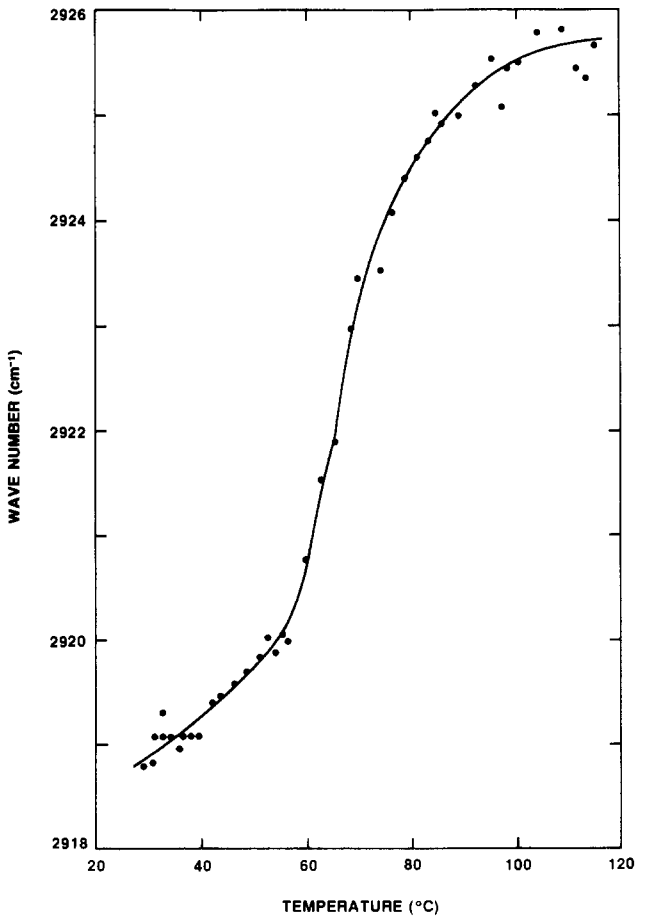

FIGURE 2: Change in maximum wavenumber of the C–H antisymmetric stretching vibration near 2920 cm^{-1} as a function of temperature. The sample is the same as Figure 1.

with a large increase in broadening apparent from 60 to 80 °C (data not shown). Finally, similar changes, albeit of smaller magnitude, were noted for the width and position of maximum absorbance for the C–H symmetric stretching peak near 2850 cm^{-1} (data not shown). In control experiments, freshly obtained samples were equilibrated at 75% rh and 22 °C. The IR results were indistinguishable from those obtained with dehydrated samples.

Samples of porcine stratum corneum treated in a manner identical with those used in the IR investigations were subjected to analysis by DSC. Figure 3 shows the DSC thermal profile obtained with a sample equilibrated at 75% rh and 22 °C. The upper trace, obtained with intact stratum corneum, shows three distinct thermal transitions occurring near 60, 70, and 95 °C, superimposed upon a broad endotherm throughout this temperature range. Thermal profiles were obtained under these same conditions for samples from eight different animals, and in all cases, these same three transitions were noted. Furthermore, freshly prepared samples yielded DSC results identical with those of dehydrated stratum corneum when both were equilibrated under equivalent conditions of temperature and relative humidity.

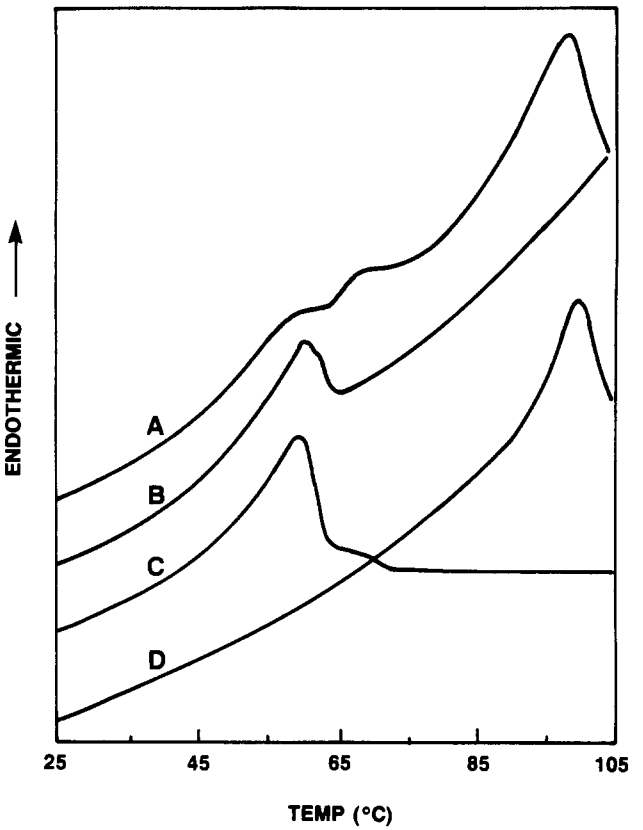

FIGURE 3: DSC thermal profiles obtained for porcine stratum corneum and lipid-extracted samples, all hydrated at 22 °C and 75% rh. Trace A represents the thermal profile obtained with an intact sample, while trace B shows the reheat profile of the same sample. Trace D shows the thermal profile of a sample after extraction with chloroform–methanol, while trace C shows the profile of the extracted material after evaporation of the chloroform–methanol solvent.

Figure 3 also shows thermal profiles obtained for reheated and lipid-extracted samples, all hydrated at 75% rh and 22 °C. The thermal profile obtained upon reheat of the initial sample (trace B) shows that the two highest temperature transitions are not present in a sample previously heated to 105 °C. In a separate experiment, a sample of stratum corneum was treated for 18 h with chloroform–methanol (2:1 v/v) in order to remove extractable lipids. The thermal profile of this lipid-extracted sample (trace D) shows only a single peak, similar to the highest temperature transition noted in the intact sample. Furthermore, reheating of this extracted sample (data not shown) resulted in a thermal profile void of any peaks. Finally, the thermal profile of the lipid extract remaining after solvent evaporation (Trace C) shows a single transition near 60 °C.

The thermal profiles of porcine stratum corneum were also investigated over a range of water contents. Samples were placed in a high relative humidity atmosphere at room tem-

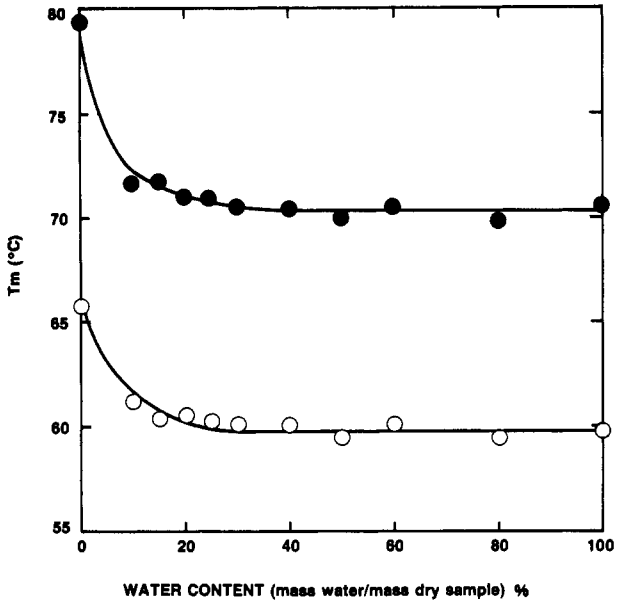

FIGURE 4: Plot of the transition temperature (T_m) of the two lowest temperature thermal transitions of porcine stratum corneum as a function of the sample water content.

perature and allowed to absorb water until the desired mass was obtained. Figure 4 shows the change in the temperature of the transition midpoint (T_m) of the two low-temperature transitions (Figure 3, trace A) as a function of the sample water content expressed as mass of water per mass of dry sample. Each point represents a separate determination with samples from one site of one animal. These results show that the T_m values of both low-temperature transitions decrease to a limiting value at water contents greater than about 20%. In contrast, the transition temperature of the highest peak shows a continuous decline in this range of water contents (data not shown).

In order to investigate the reversibility of these thermal transitions, samples of porcine stratum corneum were reheated to progressively higher temperatures. Figure 5 shows the data obtained when a sample, hydrated at 75% rh and 22 °C, was heated to 81 °C (Trace I) and then reheated to 91 °C (trace II), 115 °C (trace III), and, finally, 120 °C (trace IV). These results show that while the transition near 60 °C is invariant with prior heating, the peak occurring originally near 70 °C exhibits decreased transition temperature with each reheat. Gravimetric analysis showed no mass change of the sample during the course of these investigations.

The thermal profile of corneocyte membranes isolated from porcine stratum corneum is shown in Figure 6. These results were obtained with samples hydrated at 75% relative humidity and 22 °C. The upper trace represents the thermal profile obtained with the initial membrane preparation and shows two peaks near 60 and 70 °C. The middle trace represents the thermal profile of the same sample upon reheating and shows a transition near the low-temperature peak seen initially. The lower trace represents the thermal profile of a corneocyte membrane sample which was extracted with chloroform–methanol (2:1 v/v) for 18 h. This trace shows only a broad endotherm with no cooperative transitions.

The flux of tritated water (HTO) through porcine stratum corneum was measured over the temperature range of 22–90 °C. In all experiments, the ambient relative humidity was maintained at 75% by keeping the stratum corneum in contact with vapor above a saturated aqueous solution of NaCl. At several temperatures throughout the range investigated, flux through fresh and rehydrated samples was compared with

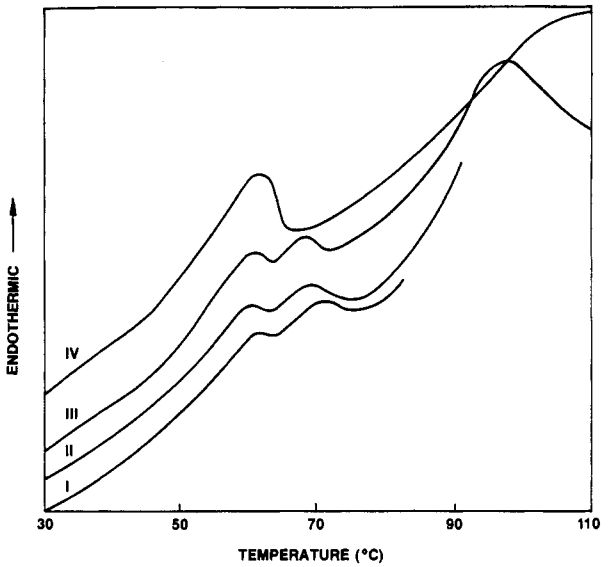

FIGURE 5: DSC thermal profile of a sample reheated to increasingly higher temperatures. The sample was heated to 81 °C (trace I) and reheated to 91 °C (trace II), 115 °C (trace III), and 120 °C (trace IV).

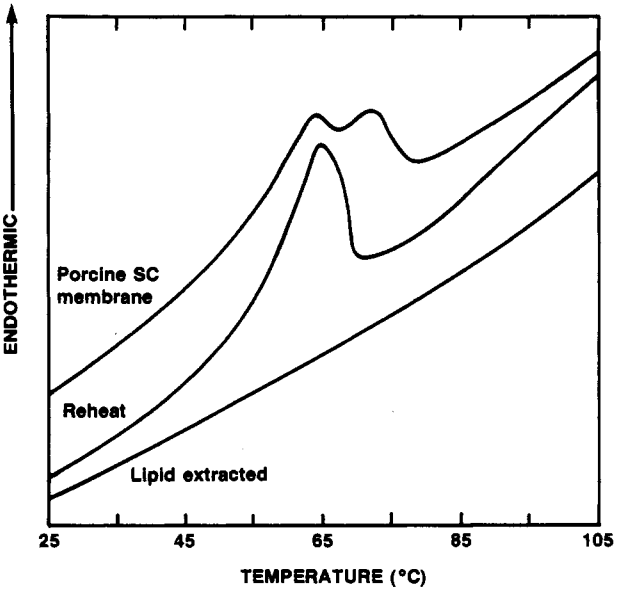

FIGURE 6: DSC thermal profiles of samples of a corneocyte membrane fraction obtained from porcine stratum corneum. All samples were hydrated in an atmosphere of 75% relative humidity and 22 °C. The upper trace represents the profile obtained with the intact membrane preparations, while the middle trace represents the reheat profile of the same sample. The lower trace represents the thermal profile of a corneocyte membrane sample after overnight extraction with chloroform–methanol (2:1 v/v).

results showing no significant difference between the two. In all determinations, at least six time points were included in the slope calculation, always yielding a correlation coefficient of greater than 0.98. The values of the permeability coefficient (k_p) vs. temperature are presented in Table I. These values represent the average and standard error of the mean obtained with samples from different animals. These results show a steady increase in k_p with increasing temperature, with relatively smaller changes occurring above 70 °C.

In order to determine the reversibility of thermally induced changes in barrier properties, the water flux was measured at 22 °C and 75 % rh, before and after the stratum corneum samples were heated. Table I shows the results of these experiments presented as the ratio of the permeability constant

Table I: Permeability Constant (k_p) for HTO Vapor Flux and K_p Ratio for after to before Heating, Both as a Function of Temperature

temp (°C)	k_p[a] (cm/h)	K_p ratio[b]
22	$(3.99 \pm 0.41) \times 10^{-4}$ (10)	1.0 ± 0.2 (9)
30	$(1.13 \pm 0.48) \times 10^{-3}$ (3)	
35		0.9 ± 0.1 (3)
40	$(1.84 \pm 0.78) \times 10^{-3}$ (3)	
50	$(3.65 \pm 1.44) \times 10^{-3}$ (3)	1.1 ± 0.1 (3)
60	$(8.02 \pm 1.76) \times 10^{-3}$ (3)	1.0 ± 0.1 (3)
70	$(2.11 \pm 0.44) \times 10^{-2}$ (4)	1.4 ± 0.3 (3)
80	$(2.78 \pm 0.20) \times 10^{-2}$ (3)	1.2 ± 0.2 (3)
90	$(3.25 \pm 0.53) \times 10^{-2}$ (4)	2.2 ± 0.5 (3)[c]
115		2.4 ± 0.5 (3)[c]

[a] The value represents the average and standard error of the mean (±SEM), with the number of determinations, each run in triplicate, noted in parentheses. [b] The average value ± SEM of the ratio of k_p after heating to the value obtained before heating as a function of heating temperature. The number of determinations is noted in parentheses. All experiments were run at 22 °C and 75% rh. [c] Significantly different from unity ($p > 0.95$) using a one-tailed t test.

at 22 °C [$k_p(22)$] obtained after the samples were heated to the $k_p(22)$ value obtained before heating vs. the heating temperature. These results show that for temperatures up to 80 °C, heating results in no change in $k_p(22)$ values. In contrast, a significant increase in $k_p(22)$ was noted for samples heated to temperatures above 80 °C.

Discussion

The results of Figure 1 show the IR spectra for porcine stratum corneum in the region associated with carbon–hydrogen (C–H) stretching vibrations. These spectra show that heating of the sample results in a blue shift and broadening of these C–H absorbances. When plotted as a continuous function of temperature (Figure 2), the results show a large increase in the wavenumber of maximum absorbance between about 60 and 80 °C, with relatively less increase at temperatures above and below this region. A plot of bandwidth vs. temperature shows similar results, with a large increase between 60 and 80 °C, but relatively little change at temperatures above 80 or below 60 °C (data not shown). We have previously shown that similar results obtained with human samples can be attributed to thermal transitions in the stratum corneum lipids (Golden et al., 1986). Thermally induced increases in peak width and wavenumber of C–H absorbance have been noted for a large variety of synthetic and biological membrane systems and have been shown to be due to increased motional freedom and the amount of gauche conformers, respectively, of lipid hydrocarbon chains undergoing thermal phase transitions (Cameron et al., 1983). Thus, the results presented here suggest that the lipids of the porcine stratum corneum undergo thermal transitions between about 60 and 80 °C.

The results of DSC experiments also provide information of thermal transition in porcine stratum corneum samples. The results of Figure 3 show three distinct transitions occurring near 60, 70, and 95 °C in samples prepared identically with those used in the IR experiments. On the basis of arguments presented for nearly identical data obtained with human samples (Golden et al., 1986), along with the results presented below, these transitions can be assigned to components of the stratum corneum.

The highest temperature transition (near 95 °C for samples equilibrated at 75% rh and 22 °C) is due to the thermal denaturation of intracellular keratin. This peak is not thermally reversible (Figure 3, trace B), as expected for a protein denaturation. Furthermore, it is present following solvent treatment of the stratum corneum (Figure 3, trace D), a process known to remove intercellular lipids with little or no extraction of highly cross-linked keratin. Finally, the high-temperature transition is absent from a corneocyte membrane preparation (Figure 6, upper trace), which is lacking intracellular keratin due to exhaustive alkali extraction (Matoltsy & Matoltsy, 1966).

The middle temperature peak (near 70 °C for samples equilibrated at 75% rh and 22 °C) exhibits thermal properties characteristic of both proteins and lipids. As shown by the thermal profiles in Figures 3 and 5, this transition, like the higher temperature keratin transition, is not thermally reversible. Nevertheless, as shown by the results of Figure 4, the T_m decreases to a limiting value with increasing water content, behavior characteristic of numerous water–lipid systems (Chapman, 1975). In addition, treatment of the sample with lipid solvents removes this transition from the thermal profile (Figure 3, trace D), suggesting lipid contribution to this peak. Since a similar transition is seen in the corneocyte membrane preparation comprised of membrane fragments and associated lipids (Matoltsy & Matoltsy, 1966), it is quite possible that this peak results from a thermal transition of a corneocyte membrane protein–intercellular lipid complex. According to this model, the intercellular lipids near the membrane boundary are stablized by nearby proteins, thus resulting in an increased T_m relative to bulk intercellular lipid. Similar stabilizing effects have been noted for membrane protein–lipid interactions in a large number of other biological systems (Chapman, 1975). This model predicts that the transition would display both lipid and protein properties, in agreement with data presented here.

The lowest temperature peak is due to thermal transitions in the intercellular lipids. Like all lipid thermotropic transitions (Chapman, 1975), this one is thermally reversible. Furthermore, as is characteristic for a variety of lipid–water systems, there is a decrease in the transition temperature to a limiting value with increasing water content (Figure 4). In addition, the peak is present in a corneocyte membrane preparation (Figure 6), and hence not associated with intracellular keratin. Finally, the peak is absent in chloroform–methanol-treated samples (Figure 3, trace D), a technique known to extract intercellular lipids.

Regardless of the precise assignment of these thermal transitions, the peaks near 60 and 70 °C reflect stratum corneum lipid structure. Recent DSC results have shown that treatment of porcine stratum corneum with lipid-fluidizing agents alters only these transitions, while the highest temperature transition is unchanged (Golden et al., 1987). Thus, these DSC results (Golden et al., 1987), combined with those presented here, strongly suggest that the transitions near 60 and 70 °C occurring in porcine samples are associated with stratum corneum lipids. When combined with the thermal IR results for similarly prepared samples (Figures 1 and 2), it can be concluded that stratum corneum lipids undergo thermally induced structural alterations in the temperature range of 60–80 °C. Furthermore, the IR results show that the structure alteration involves increased motional freedom of the lipid hydrocarbon chains, often referred to as increased lipid fluidity.

The flux of tritated water (HTO) through porcine stratum corneum was measured from 22 to 90 °C under conditions of constant ambient relative humidity. These data (Table I) show an average k_p of 1.1×10^{-3} cm/h at 30 °C and 75% rh, results similar in magnitude and variance to those obtained by Blank and co-workers for human stratum corneum under similar conditions (Blank et al., 1984). Thus, porcine and human

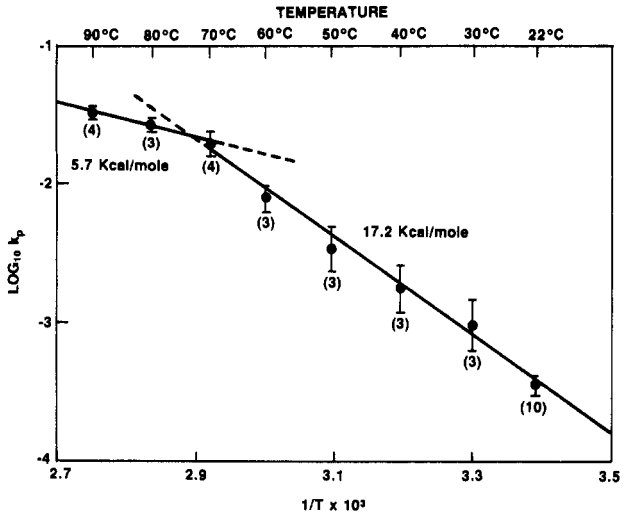

FIGURE 7: Arrhenius plot of the data of Table I, plotted as the logarithm of k_p vs. reciprocal absolute temperature.

stratum corneum appear to have similar water permeabilities, in agreement with results of Galey et al. (1976). In addition, in the physiologically relevant range of temperature, our results show an approximate doubling in HTO flux with each 10 °C increase in temperature, in close agreement with numerous in vitro and in vivo measurements of water flux through human skin over this same temperature range (Pinson, 1942; Mali, 1955; Scheuplein, 1965; Grice & Bettley, 1967; Spruit & Herweyer, 1967; Lamke & Weden, 1971). In marked contrast, however, our results obtained above 70 °C show only an approximate 25% increase in flux with each 10 °C increase in temperature.

Information regarding the mechanisms involved in temperature-dependent processes can often be derived from an Arrhenius plot of the data. The data from Table I are presented in Figure 7 as an Arrhenius plot of logarithmic k_p vs. reciprocal absolute temperature. The slope of these data yield an estimate of the activation energy for permeation of HTO through porcine stratum corneum.

The data of Figure 7 describe biphasic behavior of the change in log k_p vs. $1/T$. For all data obtained at 70 °C or below, the slope of the best-fit line yields an activation energy of 17.2 kcal/mol, in excellent agreement with the values of 14.2 kcal/mol obtained for human stratum corneum over the range of 5–50 °C (Scheuplein & Blank, 1971) and 15.4 kcal/mol obtained for intact human skin from 30 to 65 °C (Allenby et al., 1969). In contrast, at temperatures of 70 °C or above, the activation energy is 5.7 kcal/mol, very near the value obtained by Scheuplein and Blank (1971) for delipidized stratum corneum (6.3 kcal/mol) and only slightly higher than that for the free diffusion of water (4.6 kcal/mol). These latter results, when combined with the results presented here, suggest that above about 70 °C the barrier properties of the stratum corneum are comparable to those of a lipid-deficient sample, offering little resistance to the free diffusion of water.

Additional information on stratum corneum barrier properties can be derived from thermal reversibility results. As shown by the k_p ratio results in Table I, samples heated to temperatures up to 80 °C and then cooled to room temperature maintain the barrier properties of an unheated sample. In contrast, samples preheated to temperatures above 80 °C exhibit increased water flux relative to the unheated samples, indicative of an irreversible thermal alteration of barrier properties. Similar results were obtained by Allenby et al. (1969), who showed that the electrical impedance of human skin was inversely related to water flux and decreased irreversibly at temperatures above about 75 °C. Interestingly, the DSC results shown in Figure 5 also suggest that thermal irreversibility occurs for samples heated above this temperature.

These results suggest that different processes are involved in water permeation through porcine stratum corneum at temperatures above and below about 70 °C. In particular, at temperatures above 70 °C, permeation is characterized by a process with an activation energy only slightly above that of free water diffusion, while at temperatures below 70 °C the process requires about 17 kcal/mol activation energy. One possible explanation of these results is that the permeability of the stratum corneum increases with temperature to a point where unstirred layers adjacent to the sample become the primary diffusional resistance. While such effects can be important in the liquid phase where diffusion is relatively slow, these effects are much less likely in the vapor phase. Furthermore, the unstirred layer thickness (t) can be estimated from k_p and diffusivity (D) values by the relationship $t = D/k_p$ (Fettiplace & Haydon, 1980). Using our k_p values (10^{-2} cm/h at 70 °C) and a diffusivity value of 10^{-4} cm^2/s for water vapor diffusion at 70 °C, we calculated a thickness of about 30 cm. This value is clearly inconsistent with the experimental setup, and thus, the abrupt change in vapor permeability cannot be explained by unstirred layer effects.

The DSC and IR results show that porcine stratum corneum undergoes a transition involving dramatically increased lipid fluidity near 70 °C, suggesting a correlation between stratum corneum lipid structure and water flux. A similar hypothesis was advanced to explain the biphasic nature to an Arrhenius plot for water flux through frog egg (Mild & Lovtrup, 1974) and tracheal epithelial membranes (Worman et al., 1986). The correlation between lipid structure and flux of small molecules through the stratum corneum is also supported by the results of several other investigations. For example, in vitro and in vivo water flux is dramatically enhanced following treatment of the stratum corneum with lipid solvents (Blank, 1952; Onken & Moyer, 1963; Smith et al., 1982; Bowser & White, 1985). Furthermore, Elias and co-workers have shown that variations in transdermal water flux at different sites on the human body correlate inversely with the total epidermal lipid content at each site (Elias et al., 1981). These results show increases in water flux due to reduction in stratum corneum lipid content but provide little insight into structural alteration. More structurally relevant results come from Knutson and co-workers, who have shown that the flux of hydrocortisone through intact hairless mouse skin increased by several orders of magnitude between 10 and 70 °C but showed little further increase from 70 to 90 °C (Knutson et al., 1985). Since a lipid phase transition occurred at 70 °C in dehydrated stratum corneum samples from the same animal, they concluded that flux changes could reflect the structural changes accompanying the phase transition. Finally, results from our laboratory (Golden et al., 1986) and others (Goodman & Barry, 1985) have shown that certain molecules which result in enhanced flux of coapplied drug through the skin cause disruption of stratum corneum lipids.

Changes in lipid structure responsible for increases in water flux with increasing temperature may not be strictly thermal in nature. The results of several investigations have shown that the stratum corneum will absorb increasing amounts of water with increasing temperature when maintained at constant ambient relative humidity. Furthermore, water flux increases with increasing stratum corneum water content

(Blank et al., 1984). In addition, increased water content has been shown to alter DSC thermal profiles and IR spectra of stratum corneum lipids in a manner consistent with disruption of lipid structure (Knutson et al., 1985). Thus, increased lipid disorder with increased temperature under conditions of constant ambient relative humidity could be, in part, due to increased water content of the sample. Spencer et al. have made precise measurements of water uptake by human stratum corneum over the temperature range of about 20–40 °C and found an activation energy of about 5 kcal/mol at 75% ambient relative humidity (Spencer et al., 1975). This value is less than the 17 kcal/mol value obtained here for water flux in the same temperature range and suggests that at near-physiological conditions, thermally induced increases in water content contribute minimally to increased stratum corneum water permeability.

Several investigators (Elias, 1982; Wertz & Downing, 1982) have suggested that the high resistance of the stratum corneum to water flux is due to the extended multilamellar lipid domains present intercellularly in this tissue. According to this hypothesis, water moleucles must traverse the hydrocarbon regions of these lamellae in order to diffuse across this barrier. The diffusion of water molecules through hydrocarbon domains has been measured in a variety of lipid bilayers and liposomes (Boehler et al., 1978, Worman et al., 1986), yielding activation energies for water flux similar to the value reproted here for stratum corneum. Thus, the results presented here strongly suggest that water flux through the stratum corneum is limited by diffusion through the ordered hydrocarbon domain of the intercellular lipids. Our data suggest that increases in stratum corneum temperature up to about 70 °C cause increased thermal motion of the lipid hydrocarbon chains, in turn allowing greater water flux across these domains. At temperatures above about 70 °C, stratum corneum lipids appear to undergo a phase transition which renders the tissue highly permeable to water.

The irreversible changes in water flux values and DSC thermal profiles seen in samples heated above the lipid transition temperatures suggest that stratum corneum proteins may also contribute to ultimate barrier integrity. In particular, results presented here suggest that proteins associated with the corneocyte membrane may stabilize nearby intercellular lipids, and thereby contribute to water barrier properties.

In conclusion, results presented here strongly support the idea that intercellular lipid structure is primarily responsible for stratum corneum water barrier properties. In particular, increases in the fluidity of the hydrocarbon chains of lipids comprising the intercellular lamellae result in increased water flux. In light of this conclusion, it is interesting to speculate on the role of abnormal lipid structure in those dermatological disorders associated with increased transepidermal water loss (Feingold et al., 1986).

References

Allenby, A. C., Fletcher, I., Schrock, C., & Tees, T. F. S. (1969) *Br. J. Dermatol. 81, Suppl. No. 4*, 31–39.

Blank, I. H. (1952) *J. Invest. Dermatol. 18*, 433–440.

Blank, I. H., Moloney, J., Emslie, A. G., Simon, I., & Apt, C. J. (1984) *J. Invest. Dermatol. 82*, 188–194.

Boehler, B. A., De Gier, J., & Van Deenen, L. L. M. (1978) *Biochim. Biophys. Acta 512*, 480–488.

Bowser, P. A., & White, R. J. (1985) *Br. J. Dermatol. 112*, 1–14.

Cameron, D. G., Kauppinen, J. K., Moffatt, D. J. & Mantsch, H. H. (1982) *Appl. Spectrosc. 36*, 245–250.

Cameron, D. G., Martin, A., & Mantsch, H. H. (1983) *Science (Washington, D.C.) 219*, 180–182.

Chapman, D. (1975) *Q. Rev. Biophys. 8*, 185–235.

Elias, P. M. (1982) *J. Invest. Dermatol. 80*, 44s–49s.

Elias, P. M., Goerke, J., & Friend, D. S. (1977) *J. Invest. Dermatol. 69*, 535–546.

Elias, P. M., Cooper, E. R., Korc, A., & Brown, B. A. (1981) *J. Invest. Dermatol. 67*, 291–301.

Feingold, K. R., Brown, B. E., Lear, S. R., Moser, A. H., & Elias, P. M. (1986) *J. Invest. Dermatol. 87*, 588–591.

Fettiplace, R., & Haydon, D. A. (1980) *Physiol. Rev. 60*, 510–550.

Galey, W. R., Lonsdale, H. K., & Nacht, S. (1977) *J. Invest. Dermatol. 67*, 713–717.

Golden, G. M., Guzek, D. B., Harris, R. R., McKie, J. E., & Potts, R. O. (1986) *J. Invest. Dermatol. 86*, 255–259.

Golden, G. M., McKie, J. E., & Potts, R. O. (1987) *J. Pharm. Sci. 72*, 25–28.

Goodman, M., & Barry, B. W. (1985) *J. Pharm. Pharmacol. 37*, 80p.

Grice, K., & Bettley, F. R. (1967) *Br. J. Dermatol. 79*, 582–588.

Knutson, K., Potts, R. O., Guzek, D. B., Golden, G. M., McKie, J. E., Lambert, W. J., & Higuchi, W. I. (1985) *J. Controlled Release 2*, 67–87.

Lamke, L. O., & Weden, B. (1971) *Acta Derm.-Venereol. 51*, 111–119.

Mali, J. W. H. (1955) *J. Invest. Dermatol. 27*, 451–459.

Matoltsy, A. G., & Matoltsy, M. N. (1966) *J. Invest. Dermatol. 46*, 127–129.

Michaels, A. S., Chandrasekaran, S. K., & Shaw, J. E. (1975) *AIChE J. 21*, 985–996.

Mild, K. H., & Lovtrup, S. (1974) *Biochim. Biophys. Acta 373*, 383–396.

Onken, H. D., & Moyer, C. A. (1963) *Arch. Dermatol. 87*, 584–590.

Pinson, E. A. (1942) *Am. J. Physiol. 187*, 492–503.

Scheuplein, R. J. (1965) *J. Invest. Dermatol. 45*, 334–346.

Scheuplein, R. J., & Blank, I. H. (1971) *Physiol. Rev. 57*, 702–747.

Smith, W. P., Christensen, M. S., & Nacht, S. (1982) *J. Invest. Dermatol. 78*, 7–11.

Spencer, T. S., Linamen, C. E., Akers, W. A., & Jones, H. E. (1975) *Br. J. Dermatol. 93*, 159–164.

Spruit, D., & Herweyer, H. E. (1967) *Dermatologica 134*, 364–370.

Stubbs, C. D. (1983) *Essays Biochem. 19*, 1–39.

Wertz, P. M., & Downing, D. T. (1982) *Science (Washington, D.C.) 217*, 1260–1261.

Worman, H. J., Brasitus, T. A., Dudeja, P. K., Fozzard, H. A., & Field, M. (1986) *Biochemistry 25*, 1549–1555.